

# Compressive performance of masonry columns confined with highly ductile fiber reinforced concrete (HDC)

Mingke Deng<sup>1</sup>, Tong Li<sup>\*,1</sup>, Yangxi Zhang

School of Civil Engineering, Xi'an University of Architecture and Technology, Xi'an 710055, China



## HIGHLIGHTS

- The effectiveness of HDC system used to confine masonry was studied.
- The HDC as binding mortar clearly improved the deformability rather than strength.
- The HDC jacket could increase both the strength and deformability.
- Analytical model was proposed for predicting strength of confined masonry.

## ARTICLE INFO

### Article history:

Received 21 November 2019  
Received in revised form 21 February 2020  
Accepted 17 April 2020

### Keywords:

Highly ductile fiber reinforced concrete (HDC)  
Masonry columns  
Confinement  
Analytical model

## ABSTRACT

This work presents the results of an experimental investigation on the compressive behavior of clay brick masonry columns confined with highly ductile fiber reinforced concrete (HDC). The study aims to prove the effectiveness of the proposed confinement technique and detect the efficiency of different confinement forms of HDC, including internally-placed HDC which was used as binding mortar in the joints (i.e. internal HDC mortar) and external HDC jacket. Furthermore, the effect of confinement materials is examined. Analysis of the failure mode, axial load–displacement curves, peak load and ductility reveals that internal HDC mortar could considerably improve the deformability of masonry columns. Although the external HDC jacket could increase the load carrying capacity and deformability, the detachment between the external layer and masonry substrate is observed at the post-peak stage. Contribution of cement-based mortar jacket to the masonry columns is merely enhancing the load carrying capacity rather than deformability, which was caused by its quite low tensile strength. Moreover, based on the theories of mesh-reinforced brick masonry and steel tube confined concrete, analytical models available in the literatures are adopted to predict the compressive strength of HDC systems confined masonry columns. The calculation model gives a better approximation to predict the compressive strength of confined masonry columns but should need further experimental data in the future other than those adopted in this paper to verify the accuracy and reliability.

© 2020 Elsevier Ltd. All rights reserved.

## 1. Introduction

When unreinforced masonry (URM) columns are subjected compressive load, transverse expansion occurs on the masonry. In general, the lateral deformation of mortar is larger than that of brick units due to the different stiffness of two materials and great bond behavior between them. Hence, the brick units are placed in a state of bilateral tension coupled with axial compression [1,2], inducing that vertical cracks appear and propagate quickly. Consequently, multiple reinforcing techniques have been adopted for

masonry columns to improve the strength and deformability by confining transverse expansion of masonry. Some of approaches belong to the class of internal confinement, including internally-placed steel plates or steel grids in the mortar joints which are used during construction as a composite masonry structure. Other techniques belong to the class of external confinement, such as steel wrapping, steel wires hooping, fiber reinforced polymer (FRP) wrapping, and fiber reinforced cementitious mortar (FRCM) jacket. The purpose of using these approaches is to strengthen existing masonry columns.

The internal confinement by placing steel plates in the mortar joints was first proposed by Priestley and Bridgeman in 1974 [3]. They observed that steel plates restrained the transverse expansion of masonry and decreased the differential deformation between

\* Corresponding author.

E-mail address: [tongli@xauat.edu.cn](mailto:tongli@xauat.edu.cn) (T. Li).

<sup>1</sup> These authors contributed equally to this work.

the brick units and mortar. Ewing and Kowalsky [4] investigated the compressive behavior of grouted clay brick masonry prisms confined with internally-placed thin galvanized steel plates in the mortar joints. It was noted that confinement plates effectively enhanced the strength and deformability of masonry prisms, and the experimental stress–strain curves agreed well with the modified Kent–Park model. Campione et al. [5] studied the effect of steel grids placed in the mortar joints on the compressive behavior of brick masonry columns tested under concentric and eccentric loads. Researchers summarized that internal confinement could be used to reconstruct a new construction by conventional techniques.

Multiple studies on the externally-confined masonry columns have been carried out in the past. Ouyang and Liu [6] adopted steel wrapping for confining masonry columns and proposed the analytical model for predicting compressive strength. Using steel cords or steel wires hooping to confine masonry columns were investigated by Borri et al. [7] and Campione et al. [8]. They observed that steel cords hooping could considerably improve the deformability rather than strength.

In the last two decades, the application of FRP wraps has been adopted for confining masonry columns, and this technique was derived from confinement method applied to concrete members. One of the first investigations on the FRP-confined masonry columns was carried out by Kreaikas and Triantafyllou [9] in 2005. Researchers observed that FRP confinement increased both the strength and deformability of masonry columns, and provided a simple confinement model to predict the strength and ultimate strain. Afterwards, further studies [10–16] on the FRP-confined masonry columns have been carried out including following variables: masonry materials, number of FRP layers, cross-section aspect ratio, high-depth ratio of prism, radius at corner, and type of fibers. El-Sokkary and Galal [17] carried out the eccentric loading tests on the reinforced concrete masonry columns confined with FRP wraps, and provided analytical model to predict the axial capacity of the tested members. From a theoretical point of view, Minafò et al. [18] compared the main existing theoretical models to predict the compressive stress–strain curves of FRP-confined masonry. However, several critical issues have been found in the application of FRP wraps, including poor fire resistance of organic matrix, stress concentration near the sharp corner, poor bond behavior at high temperature or on a wet surface, and brittle failure of FRP.

An alternative technique to overcome aforementioned limitations is the use of fiber reinforced cementitious mortar (FRCM) composite, also known as textile reinforced mortar (TRM) and textile reinforced concrete (TRC), where the organic matrix has been replaced with cementitious mortar. One of the introductory studies on the FRCM-confined masonry columns was performed by Yilmaz et al. [19] in 2013, who tested some clay brick masonry columns confined with mortar or basalt FRCM jacket. The results indicated that mortar-confined specimens showed similar behavior with control specimens, while FRCM jacket provided a limited increase in strength but substantial gains in deformability and energy dissipation. Cevallos et al. [20] tested masonry elements strengthened with flax or polyparaphenylene benzobisoxazole (PBO) FRCM composites and subjected to eccentric load. The results revealed that both the flax- and PBO-FRCM systems increased the strength and deformability of masonry elements. Moreover, flax fabric exhibited a greater bond behavior with masonry substrate than PBO fabric. Minafò and La Mendola [21] studied the effect of mortar grade on the compressive behavior of FRCM-confined masonry columns. Researchers provided three simplified models to predict the tensile constitutive law of FRCM composite. Additionally, based on a suitable tensile constitutive law of FRCM, an iterative procedure was proposed for predicting the compressive behavior of FRCM-

confined masonry columns. Kreaikas [22] investigated the effect of cross-section aspect ratio, number of TRM layers, and corner radius on the carbon fiber TRM confined masonry columns. Fossetti and Minafò [23] carried out comparative tests on the masonry columns confined with FRP wrapping, FRCM jacket, and steel wires hooping on the mortar joints and provided analytical models to predict the compressive strength of different techniques confined masonry.

The above survey of literatures indicates that the application of different confinement forms and materials to improve strength and ductility of masonry columns have been proved. However, few studies have been reported on the masonry columns confined with fiber reinforced cementitious composite, such as engineered cementitious composites (ECC) [24–26], strain hardening cementitious composite (SHCC) [27,28] and highly ductile fiber reinforced concrete (HDC) [29–31], which exhibited strain-hardening behavior in tension and high toughness in compression. Therefore, the present paper aims to investigate the effect of HDC on the compressive behavior of masonry columns by using aforementioned two different confinement forms. Fifteen specimens, including twelve confined and three unconfined columns, are tested under monotonic concentric load up to failure. Confinement forms (internal and external confinement) and materials (HDC and cement-based mortar) are varied to explore the effectiveness of the HDC confinement in terms of failure mode, axial load–displacement curves, peak load and ductility. Moreover, based on the theories of mesh-reinforced brick masonry and steel tube confined concrete, analytical models available in the literatures are used to predict the compressive strength of HDC systems confined masonry.

## 2. Experimental program

### 2.1. Specimen description and preparation

The experimental program consisted of fifteen clay brick masonry columns tested under axial compression load. The nominal dimensions of the specimens were  $b = 240 \text{ mm} \times h = 370 \text{ mm} \times L = 720 \text{ mm}$  (aspect ratio  $L/b = 3$ ). Each specimen was composed of clay brick units placed in twelve rows with eleven mortar bed joints in between, as shown in Fig. 1. The average thickness of mortar joints was 10 mm. The test parameters were confinement forms and materials, which were summarized in Table 1. The internal confinement form was accomplished by replacing cement-based mortar with HDC mortar. When HDC is subjected to the compressive load, propagation of vertical cracks and lateral deformation are restrained by the fiber bridging stress induced by the bridging effect of polyvinyl alcohol (PVA) fibers. Moreover, the fiber bridging stress is stable and sustained after the first crack opening due to the strain-hardening behavior in tension. Thus, confinement force provided by the fiber bridging stress, as expressed in Fig. 2, is similar to the stirrup confinement stress in the reinforced concrete members. In other words, PVA fibers could be deemed to confine a number of stirrups, as discussed in Ref. [31]. In this case, internally-placed HDC mortar could be considered that transverse reinforcements are placed in the mortar joints.

All the masonry columns were classified into five sets with three identical specimens per set to consider the experimental scatter usually noticed in the masonry structures. Set 1 was unconfined masonry columns named UC. Set 2 was confined with cement-based mortar jacket, and sets 3–5 were confined with HDC systems. The confined specimens are given a nomenclature as M–X–Y–Z, where M indicates confined masonry columns, X refers to internal confinement materials (U for cement-based mortar indicating no internal confinement, H for HDC mortar), Y designates external confinement materials (U for no external confine-

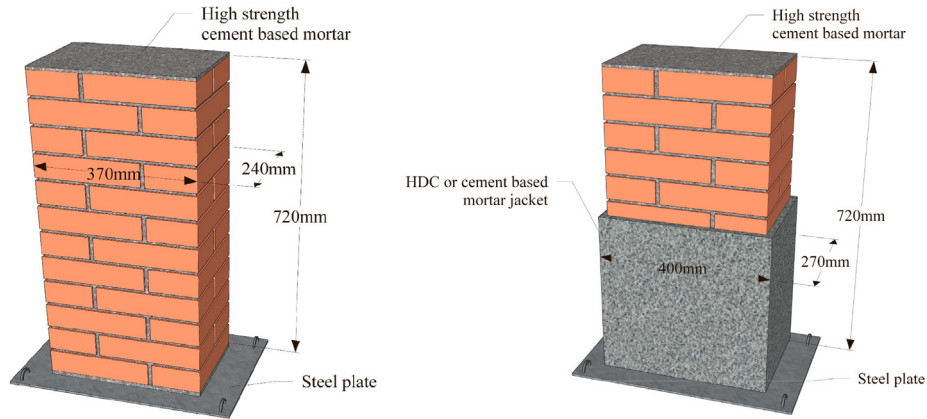


Fig. 1. Geometry of the specimen.

Table 1  
Properties of the specimens.

Set	Area of cross section (mm <sup>2</sup> )	Confinement materials	Confinement forms Internal mortar	External jacket
UC	240 × 370	None	×	×
M-U-C	240 × 370	Cement-based mortar	×	✓
M-H-U	240 × 370	HDC	✓	×
M-U-H	240 × 370	HDC	×	✓
M-H-H	240 × 370	HDC	✓	✓

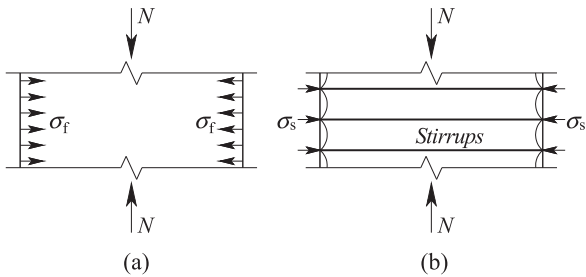


Fig. 2. Confinement stress provided by: (a) fiber bridging stress; (b) stirrups.

ment, C for cement-based mortar jacket and H for HDC jacket), and Z refers to the number of replicate. For example, specimen M-U-H-2 is the second masonry column confined with external HDC jacket and no internal confinement. All masonry columns were manufactured on the 5 mm-thickness steel plates with four rings.

The first step for preparing all specimens was manufacturing URM columns and internally-placed HDC mortar confined masonry columns. After a curing time of 7 days, the steps taken to jacket the masonry columns were taking dust away from surface, wetting prisms, installing the external confining jackets. After that, the top surfaces of all specimens were capped with 15 mm-thickness high strength cement-based mortar to ensure the horizontality of the columns and obtain uniform load distribution in the test. Finally, each specimen was cured a further time of 56 days before tested in the laboratory.

2.2. Material properties

Solid clay brick units with the nominal dimensions of 240 × 115 × 53 mm were used to assemble the masonry columns. The compressive strength of the bricks, determined by uniaxial compressive tests on ten specimens in terms of GB/T 2542-2012 Test Methods for Wall Bricks [32], was equal to 8.87 MPa.

The mortar used for binding the masonry columns and external confinement jackets was cement-based mortar (cement: sand: water ratio of 1:4.57:1.1 by weight). The compressive strength of mortar, obtained by means of compressive tests on 12 standard 70.7 mm cubes in accordance with JGJ/T 70-2009 Standard for Test Method of Basic Properties of Construction Mortar [33], was equal to 17.19 MPa. It should be noted that the compressive strength of mortar used to construct URM columns was relatively higher than that used in the old masonry structures. However, the aim of the present paper was to evaluate the efficacy of the HDC systems for confining masonry columns subjected to concentric load. Hence, the interaction between confinement material and masonry substrate was a main parameter to evaluate this composite as a confinement system for the old masonry structures [20].

Additionally, the HDC mix utilized in this study consisted of cement, fly ash, sand and water, with corresponding proportions of 1:1:0.72:0.58 by the weight of the cement. The content of high-range water reducers was 8 kg/m<sup>3</sup> and the volume content of PVA fibers was 2%. The mechanical behavior of PVA fiber was reported in Table 2. The average compressive strength of HDC, verified by the compressive tests on twelve standard 70.7 mm cubes, was equal to 54.60 MPa. In terms of Ref. [34], the uniaxial compressive strength of HDC was 48.05 MPa. The tensile behavior of HDC was obtained by the direct tensile tests on three dog-bone-shaped specimens with dimension of 350 × 50 × 15 mm. The typical tensile stress-strain curve was plotted in Fig. 3. It is evident that HDC is characterized by the strain-hardening behavior in tension and the ultimate tensile strain of HDC can exceed 1%. The average tensile strength of HDC, obtained from tensile stress-strain curve, was equal to 6.10 MPa.

2.3. 2.3. Test setup

The test setup was shown in Fig. 4. The uniaxial compressive tests on all masonry columns were carried out by an electrohydraulic servo testing machine with a maximum load of 5000 kN. The specimens were loaded by displacement-controlled mode with

**Table 2**  
Properties of PVA fiber.

Length (mm)	Diameter ( $\mu\text{m}$ )	Tensile strength (MPa)	Elastic modulus (GPa)	Elongation (%)	Specific gravity ( $\text{g}/\text{cm}^3$ )
12	39	1600	40	7	1.3

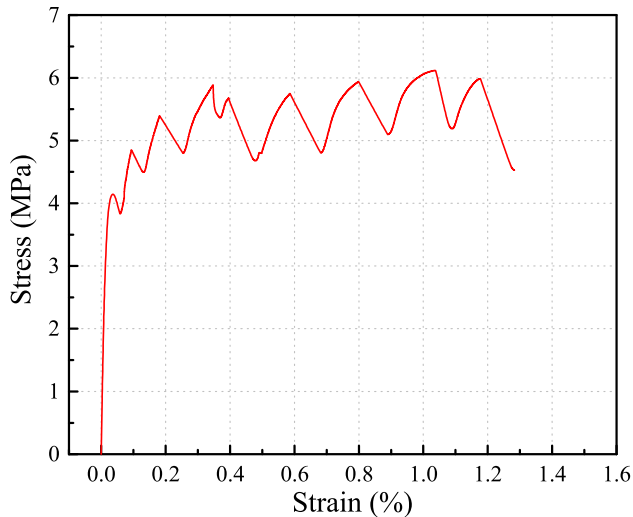


**Fig. 3.** Tensile stress–strain curve for HDC.

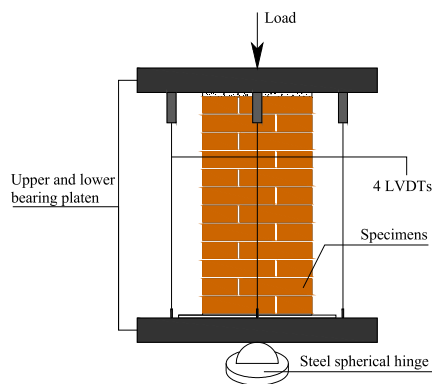


**Fig. 4.** Test setup and instrumentation for specimens.

a loading rate of 0.5 mm/min. A steel spherical hinge was placed under the lower loading platen and centered with the respect to the center of the specimen in order to obtain uniform load distribution and avoid any initial eccentricity. The force was measured by a load cell. The axial deformation was measured by four linear variable displacement transducers (LVDTs) mounted on four faces of the column between the upper and bottom loading platens and without any damage of the specimen. From the obtained real-time readings of force and deformation, the axial load–displacement diagrams for each column could be plotted. Three preload cycles were applied between 20 and 30 kN to check the correctness of installed devices.

### 3. Results and discussions

#### 3.1. Failure modes

The failure modes of some specimens are shown in Fig. 5 in order to compare the cracking patterns and the failure mechanisms for URM columns and HDC-confined masonry columns. The control

specimens exhibited a brittle behavior. As mentioned before, the mortar joints had a larger lateral deformation than the brick units under the axial compression load and, consequently, it induced tensile stress in the bricks. When the tensile strength limit of bricks was reached, the vertical cracks occurred on the specimen, and they propagated rapidly along the height of columns with the increase of axial load. This stage was short owing to the quite low tensile strength of masonry. Hence, the unconfined masonry columns were divided into two or more slender prisms by the continuous sub-vertical cracks. The URM columns failed from the slender prisms crushing or losing stability, resulting from the stress redistribution near these vertical cracks. It should be noted that the compressive strength of brick unit was not utilized adequately due to the premature rupture of bricks caused by the unconstrained transverse expansion of masonry. Although M-U-C set was confined with cement-based mortar jacket, specimens were still characterized by a sudden failure. This could be attributed to the brittle property of the cement-based mortar. The confinement jacket failed since the first vertical crack opened. Therefore, the lateral confinement force provided by mortar jacket was quite limited, leading to that the expansion of masonry core was almost not restrained after the early loading stage. The failure of M-U-C set was similar to that of control specimens.

M-H-U set, replacing cement-based mortar with HDC, failed for local brick units crushing. Indeed, M-H-U set exhibited more fine cracks on the bricks and no visible continuous vertical cracks through the columns. By contrast, for the unconfined masonry columns the vertical cracks were more open and involved the mortar joints. This cracking pattern could be explained that HDC mortar with high tensile strength and bridging effect of PVA fibers decreased the lateral deformation of brick units and restrict the propagation of vertical cracks. Therefore, HDC mortar produced a homogeneous plane behavior on the cross section and distributed the axial stress uniformly. This was different from URM columns which were divided into multiple slender prisms. As a result, M-H-U set kept integrality at failure and clearly improved the ductility.

M-U-H set was confined with external HDC jacket while M-H-H set was confined both with internal HDC mortar and with external HDC jacket. These two sets showed a similar cracking process and failed from local masonry crushing. The external confinement force provided by HDC jacket effectively inhibited the transverse expansion of masonry core, inducing that the first cracking load, strength and axial deformability of masonry columns were clearly improved. However, detachment between local HDC layer and masonry substrate was observed after the peak load, resulting from both the discontinuous distribution of short PVA fibers on the corner caused by construction technique and the stress concentration near the corner. Nevertheless, M-H-H set showed better ductility and integrality, and the masonry crushing was moderate if compared with M-U-H set. This could be attributed to the internal confinement provided by HDC mortar, leading to a homogeneous plane behavior on the cross section.

#### 3.2. Axial load–displacement curves

The axial load–displacement curves for all test masonry columns are plotted in Fig. 6. The axial force was measured by the load cell. The axial displacement was the average readings of the



**Fig. 5.** Failure modes: (a) unconfined; (b) M-U-C; (c) crushing of slender prisms; (d) M-H-U; (e) M-U-H; (f) severely crushing of masonry; (g) M-H-H; (h) moderately crushing of masonry.

four LVDTs. Specimen UC-1 has been ignored as a result of premature damage during the transport. The compressive behavior of control specimen was rather weak with low axial capacity and poor deformability. The approximate linear ascending branch was observed up to the peak load, followed by a marked slope of the softening branch up to collapse, which highlighted the brittle failure of the URM columns. Compared to the control specimens, although the peak load and initial stiffness of M-U-C set were improved, the steep softening branch after the maximum load was recorded. The specimens exhibited a poor deformability and a brittle type of failure. Moreover, from the Fig. 6(a) and (b), it is evident that the first cracking load was about half of the peak load for the UC and M-U-C sets, indicating that the cement-based mortar jacket could not effectively restrict the lateral expansion of masonry core and delay the propagation of the vertical cracks. Thus, the cement-based mortar jacket was not an effective confinement technique to enhance the deformability of URM columns.

From the axial load–displacement curve of M-H-U set, internally-placed HDC mortar could improve the compressive behavior of masonry columns with a substantial gain in deformability. A non-linear ascending branch was recorded until the peak load, highlighting a great elastic–plastic deformability. The slope of descending post-peak branch was flatter than that of UC and M-U-C sets. The strength degradation of specimens was slowed down, marked by a ductile failure. Furthermore, the first cracking

load was almost 80% of the peak load, revealing that the internal HDC mortar could decrease the lateral deformation of bricks and delay the opening of the first crack.

The HDC-jacketed masonry columns (M-U-H set) showed a non-linear ascending branch before the peak load, and followed by a rapidly descending branch up to failure. This is mainly due to the fact that the detachment between local HDC jacket and masonry substrate induced a sudden axial load drop. By contrast, M-H-H set exhibited a substantial gain both in the peak load and the deformability. The axial load–displacement curves showed a non-linear ascending branch, followed by a flatter descending branch up to failure. Although local HDC layer of M-H-H set also detached from masonry substrate after the peak load, the axial load did not drop rapidly. This is different from M-U-H set and can be attributed to the confinement of internal HDC mortar as discussed before. When the external HDC jacket detached from masonry substrate or could not continue to confine masonry core, the internal HDC mortar could restrain the expansion of brick masonry and improve the axial deformability. However, the axial load of specimen M-H-H-3 still dropped abruptly, mainly caused by the premature detachment of HDC layer due to a direct contact between HDC layer and loading platen. Additionally, the first cracking load of these two sets were more than 70% of the peak load, mainly due to the fact that external HDC jacket could restrain the lateral expansion of masonry core.

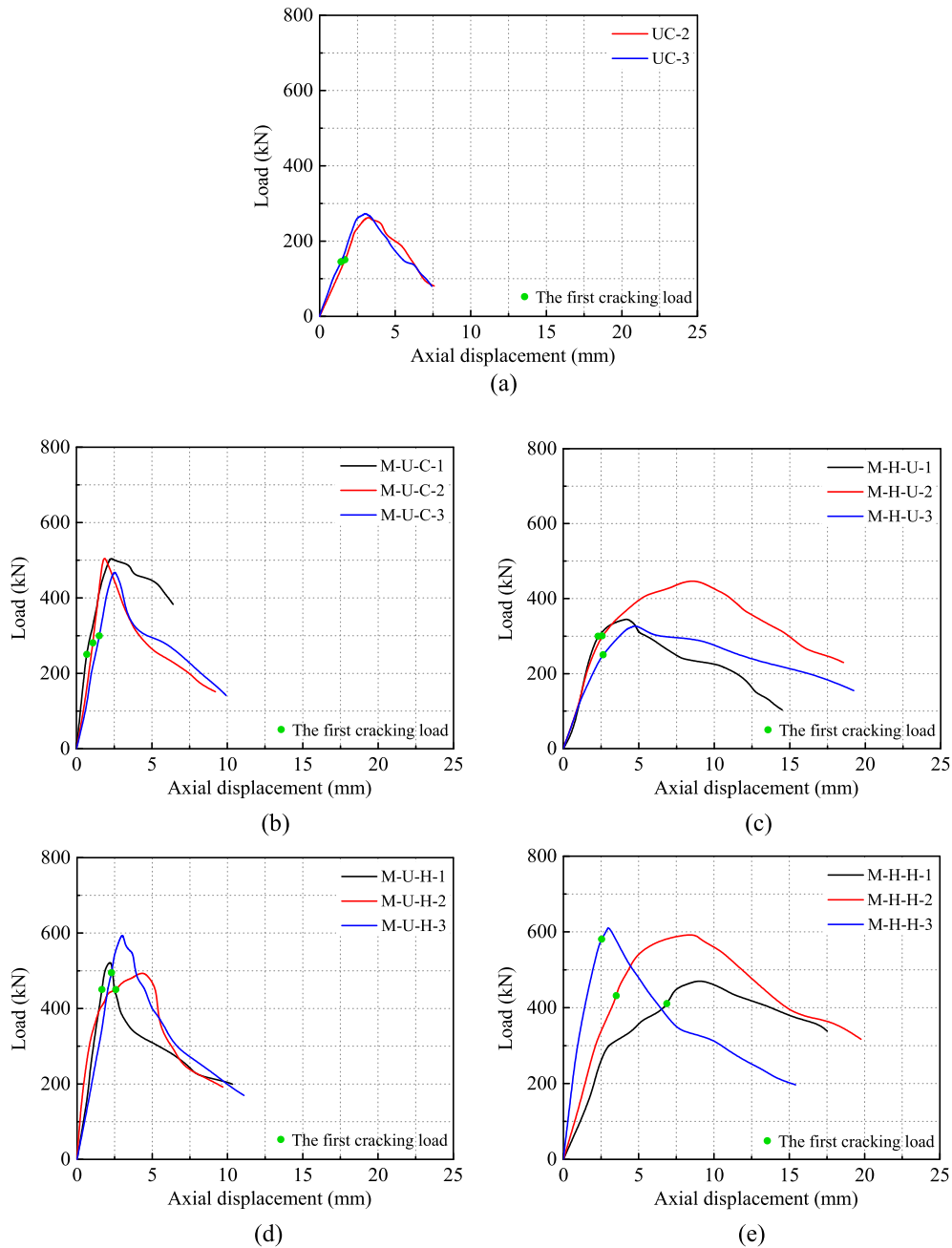


Fig. 6. Axial load–displacement curves: (a) UC; (b) M-U-C; (c) M-H-U; (d) M-U-H; (e) M-H-H.

### 3.3. Confinement mechanism of HDC

In general, the lateral deformation of mortar joints was greater than that of clay brick units when the URM columns were subjected to axial loads as mentioned before. Hence, there was the mutual confinement between the mortar and bricks, inducing the additional lateral tensile stress on the brick units. This provides an illustration as to why the first vertical crack generally opened on the brick rather than the mortar joint. Differently, the lateral expansion of HDC is less than that of cement-based mortar due to the bridging effect of PVA fibers under the same axial loads. The transverse differential deformation between the mortar and brick units was reduced by replacing cement-based mortar with HDC. In other words, HDC as binding mortar could reduce the additional tensile stress and transverse dilation of brick units. The

opening and propagation of vertical cracks were significantly delayed. Therefore, the strength and deformability of masonry columns were improved. This confinement mechanism is similar to the steel plates confined masonry columns that the confinement plates decreased the lateral expansion of the mortar joint and brick unit as shown in Ref. [4]. Furthermore, although the micro vertical cracks opened in the mortar joints, HDC mortar kept integrity owing to the bridging effect of PVA fibers. This effect could distribute the axial load uniformly and prevent masonry columns from being divided into two or more slender pieces, which is quite useful to improve the axial deformability. Accordingly, the specimens kept integrity and exhibited a ductile type of failure. Confinement stress of HDC mortar could be expressed in Fig. 7(a).

The confinement mechanism of external HDC jacket confined URM columns is shown in Fig. 7(b). The lateral tensile stress

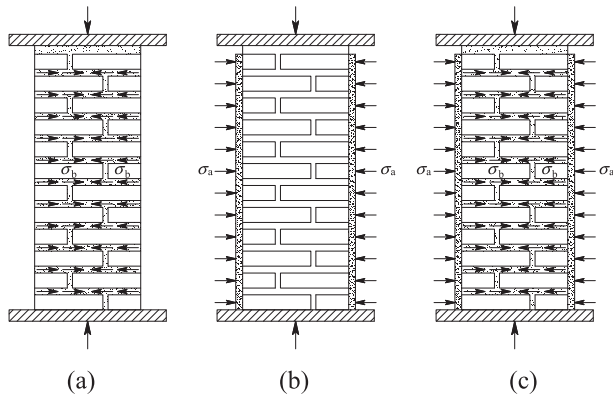


**Fig. 7.** Confinement stress: (a) HDC mortar confined; (b) HDC jacket confined; (c) combined confinement.

occurred on the HDC jacket caused by the transverse dilation of masonry core when there was no direct contact between external jacket and loading platen. In turn, the masonry core was placed in a state of triaxial compression, thus the strength and deformability of masonry were improved. The confinement force provided by HDC jacket was passive and increased with the increase of the lateral expansion until that HDC jacket failed or detached from masonry substrate. By contrast, the combined confinement of internal HDC mortar and external HDC jacket, as given in Fig. 7 (c), is stronger than that provided by the any single reinforcement method. The external HDC jacket restrained the lateral expansion of masonry core as discussed previously. Moreover, the internal HDC mortar reduced the additional tensile stress of the brick units and prevented the brick masonry severely crushing, accordingly, it delayed the external HDC jacket detaching from masonry substrate. In fact, masonry core was under a highly triaxial compression state with the combined confinement. This could be an illustration as to why the load bearing capacity and deformability of M-H-H set were significantly enhanced.

### 3.4. Peak load

The experiment results in terms of peak load, Coefficient of Variation (COV) and peak load gain are shown in Table 3 for each specimen. The peak load gain is defined as the average maximum load of confined specimens normalized to the corresponding value of the control specimens. Although the average peak load gain of M-U-C set was 84%, cement-based mortar jacket could not be an effective confinement technique because of the weak compressive behavior of M-U-C set in terms of failure modes and load–displacement curves. The fact of great peak load gain could be explained that cement-based mortar jacket supported a part of axial loads because of the bonding and frictional forces between the external jacket and the masonry substrate in spite of no axial load is applied on the external jacket directly. On the other hand, the peak load increased by 25%, 101%, and 125% for M-H-U, M-U-H, M-H-H sets compared to URM columns, respectively. Therefore, applying HDC systems are effective and alternative confinement techniques to improve the axial bearing capacity of URM columns. More discussions are reported in the following section.

### 3.5. Ductility

Based on the Ref. [35], the ductility index of masonry columns is defined as the ratio of ultimate axial displacement ( $\Delta_{mu}$ ) to its axial displacement at peak load ( $\Delta_m$ ). The ultimate axial displacement is

the corresponding displacement at 15% peak load degradation. It should be noted that although the definition of ultimate axial displacement is arbitrary, the ultimate value used in the present work is consistent with American ACI 440.2R guideline [36]. For the sake of evaluating the effect of different confinement forms on the deformability,  $\Delta_m$ ,  $\Delta_{mu}$  and ductility index of confined masonry columns were normalized to the corresponding values of control specimens, respectively, as reported in Table 4. The axial displacement at peak load, ultimate axial displacement and ductility index of M-U-C set decreased by 24%, 30% and 9%, compared to control specimens, respectively. This could be explained that cement-based mortar jacket increased the stiffness of masonry columns, but it cannot provide enough confinement forces to inhibit the transverse expansion of masonry core, leading to the reduction of deformability.

The axial displacement at peak load, ultimate axial displacement and ductility index of M-H-U set increased by 43%, 161% and 82%, respectively. However, the peak load of M-H-U set only increased by 25%, revealing that internally-placed HDC mortar could significantly improve the axial deformability and moderately increase the axial bearing capacity of masonry columns. This observation is in agreement with the internal steel grids [5] or external steel wires confined masonry columns [8,23]. This confinement form by inhibiting the transverse deformation of mortar joints exhibited the higher gain in the axial deformability comparing to the gain in strength.

M-U-H set showed a modest increase on the axial deformability. The axial displacement at peak load, ultimate axial displacement and ductility index increased by 1%, 12% and 10%, respectively. After manufacturing masonry columns, the corners were not rounded, inducing that the stress concentration near the corner was quite obvious during the loading tests. Moreover, when installing HDC jacket, it is inevitable that the distribution of PVA fibers was discontinuous on the corner. These two reasons led to an obvious detachment between the local HDC layer and masonry substrate at the post-peak stage, thus the deformability was not clearly improved.

By contrast, compared to the URM columns, the ductility index of M-H-H set only increased by 9% while the axial displacement at peak load and ultimate axial displacement increased by 183% and 207%, respectively. When internal HDC mortar and external HDC jacket were applied together, HDC systems induced a strong confinement force to the masonry core. The lateral expansion of brick masonry was restrained and the propagation of vertical cracks was delayed. Besides, the confinement provided by HDC mortar delayed the detachment between the external HDC jacket and masonry substrate. Particularly, a quite slight detachment was observed at the post-peak stage in the M-H-H set. Accordingly, combined confinement forms of internal HDC mortar and external HDC jacket could significantly improve the deformability and ductility of URM columns.

## 4. Theoretical prediction

### 4.1. Strength prediction of internal HDC mortar confined columns

Based on the aforementioned experiment results and discussion, it is clear that the reinforcement mechanism of internally-placed HDC mortar is reducing the differential deformation between the mortar joints and brick units, which could improve the compressive strength and deformability of masonry columns. This is similar to the internally-placed steel grids confined masonry columns. The confinement model is shown in Fig. 8. Thus, the calculation of compressive strength is proposed for internal HDC mortar confined masonry according to the method of mesh-reinforced

**Table 3**  
Peak load for all specimens.

Specimen number	Peak load (kN)	Average Peak load (kN)	Average strength (MPa)	COV	Normalized peak load
UC-2	264.2				
UC-3	274.3	269.3	3.03	1.9%	1.00
M-U-C-1	506.6				
M-U-C-2	510.8	496.2	5.59	3.6%	1.84
M-U-C-3	471.2				
M-H-U-1	346.0				
M-H-U-2	448.8*	337.2	3.80	2.6%	1.25
M-H-U-3	328.3				
M-U-H-1	528.1				
M-U-H-2	495.6	540.3	6.08	7.8%	2.01
M-U-H-3	597.1				
M-H-H-1	473.1*				
M-H-H-2	597.8	606.9	6.83	1.5%	2.25
M-H-H-3	616.2				

\* These values have been ignored due to the high experimental scatter.

**Table 4**  
Normalized deformation of masonry columns.

Set	$\Delta_m$ (mm)	Normalized $\Delta_m$	$\Delta_{mu}$ (mm)	Normalized $\Delta_{mu}$	Ductility index	Normalized ductility index
UC	3.17	1.00	4.12	1.00	1.30	1.00
M-U-C	2.42	0.76	2.87	0.70	1.19	0.91
M-H-U	4.55	1.43	10.74	2.61	2.36	1.82
M-U-H	3.21	1.01	4.60	1.12	1.43	1.10
M-H-H	8.96	2.83	12.67	3.07	1.41	1.09

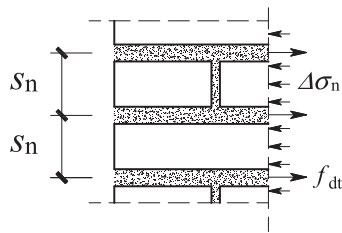


**Fig. 8.** Confinement model of HDC mortar confined masonry.

brick masonry given in the GB 50003-2011 Code for Design of Masonry Structures [37]. The lateral and axial deformation of HDC mortar confined columns are larger than that of URM columns under the axial compressive load. The added deformation can be calculated by

$$\Delta \varepsilon_n = \Delta \sigma_n / E, \quad \Delta \varepsilon = \Delta \sigma / E \quad (1)$$

where  $\Delta \varepsilon_n$ ,  $\Delta \sigma_n$  are added lateral strain and stress, respectively;  $\Delta \varepsilon$ ,  $\Delta \sigma$  are added axial strain and stress, respectively;  $E$  is the elastic modulus of masonry. Based on the Poisson's ratio, the relationship between lateral strain and axial strain can be written as follows:

$$\Delta \varepsilon_n = \nu \Delta \varepsilon \quad (2)$$

where  $\nu$  is the Poisson's ratio of masonry, which can be equal to 0.32 according to the GB 50003-2011. As shown in Fig. 8, the added lateral stress could be calculated by the equilibrium equation on the cross section in the following form:

$$\Delta \sigma_n = \frac{f_{dt} t}{S_n} \quad (3)$$

where  $f_{dt}$  is the tensile strength of HDC;  $t$  is the average thickness of HDC mortar joints;  $S_n$  is the average spacing of HDC mortar joints. Hence, the compressive strength of masonry columns confined with internally-placed HDC can be expressed by

$$f'_{cm} = f_{0m} + \Delta \sigma = f_{0m} + \frac{f_{dt} t}{\nu S_n} \quad (4)$$

where  $f'_{cm}$  is the compressive strength of HDC mortar confined masonry;  $f_{0m}$  is the compressive strength of unconfined masonry and can be calculated in terms of the GB 50003-2011.

#### 4.2. Strength prediction of external HDC jacket confined columns

The basis of the HDC jacket contribution to the strength of confined masonry is the transverse confinement stress  $\sigma_n$  developing in the masonry core in response to the jacket forces, which is analogous to confined concrete members. Therefore, the strength prediction of the external HDC jacket confined masonry will be discussed according to the steel tube confined concrete [38] and steel wrapping confined masonry columns [6] in this section. The transverse confinement stress on the rectangular cross section is presented in Fig. 9 when the peak load is reached. This stress is nonuniform in general caused by the rectangular cross section. As a result of the fact that compressive strength of confined masonry depends on the smaller confinement force, the transverse confinement stress  $\sigma_n$  can be calculated as follows:

$$\sigma_n = \sigma_{nx} = \frac{f_{dt} t_0}{h} \quad (5)$$

where  $t_0$  is the thickness of HDC jacket;  $h$  is the depth of cross section. As already done in Refs. [38,6], the compressive strength of masonry columns confined with HDC jacket can be given in the following form:

$$f_{cm} = f_{0m} \left( 1 + 1.5 \sqrt{\frac{\sigma_n}{f_{0m}}} + 2 \frac{\sigma_n}{f_{0m}} \right) \quad (6)$$

where  $f_{cm}$  is the compressive strength of HDC jacket confined masonry;  $f_{0m}$  is the compressive strength of unconfined masonry and can be calculated here by experimental results. When the compressive strength of masonry columns confined both with internal HDC mortar and with external HDC jacket is calculated,  $f_{0m}$  in Eq. (6) can be replaced with  $f'_{cm}$  in Eq. (4).

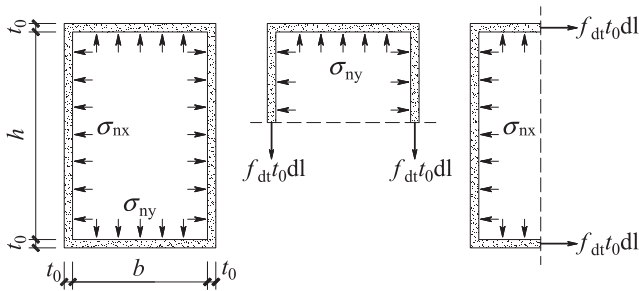


Fig. 9. Confinement model of HDC jacket confined masonry.

Table 5

Comparison between calculation and experimental values.

Set	$f_{om}$ (MPa)	$f_{cm}^{pred}$ (MPa)	$f_{cm}^{exp}$ (MPa)	$f_{cm}^{exp}/f_{cm}^{pred}$
M-H-U	1.39	3.61	3.80	1.053
M-U-H	3.03	5.84	6.08	1.041
M-H-H	3.61	6.59	6.83	1.036

#### 4.3. Comparison between predicted and tested results

Table 5 shows the comparison between predicted and experimental compressive strength for HDC systems confined masonry columns. As can be observed, the ration  $f_{cm}^{exp}/f_{cm}^{pred}$  is very close to 1 for all test members, indicating that the compressive strength of HDC confined masonry is predicted with enough accuracy. However, the results of aforementioned theoretical prediction refer to a limited number of specimens. Further studies and more experimental data are necessary to verify the reliability of the calculation model.

## 5. Conclusions

This paper presents an experimental study on the compressive behavior of concentrically-loaded clay brick masonry columns confined with HDC systems, followed by the development of a calculation model for predicting the compressive strength of confined masonry. On the basis of the results obtained and considering the limits of the analyzed variables, the conclusions can be drawn as follows:

- 1) Although cement-based mortar jacket increased the load carrying capacity of masonry columns compared to the URM columns, the deformability is quite weak. The steep softening branch after the peak load was observed, representing that the cement-based mortar jacket cannot restrain the transverse dilation of masonry core due to its low tensile strength. The confined prisms still showed a brittle failure.
- 2) HDC mortar confined masonry columns exhibit a great enhancement on the deformability compared to the URM columns, especially that specimens show a ductile type of failure with the capacity degradation slowing down in the post peak behavior.
- 3) HDC jacket effectively restricts the transverse dilation of masonry core, thus both the load carrying capacity and deformability of masonry columns are significantly improved. Although the detachment between the HDC jacket and masonry substrate is observed at the post peak stage, internally-placed HDC mortar (combined confinement) could delay the debonding behavior.

- 4) Based on the theories of mesh-reinforced brick masonry and steel tube confined concrete, the calculation model is proposed for predicting the compressive strength of HDC systems confined masonry. Predicted values are consistent with experimental results.

Finally, the aforementioned experimental results and discussions proved that HDC systems are efficient and alternative techniques to improve the load carrying capacity and deformability of the clay brick masonry columns. However, further experimental studies are needed in the future including masonry materials, cross-section aspect ratio, and thickness of HDC jacket to generalize the findings.

## 6. Author statement

All persons who meet authorship criteria are listed as authors, and all authors certify that they have participated sufficiently in the work to take public responsibility for the content, including participation in the concept, design, analysis, writing, or revision of the manuscript. Furthermore, each author certifies that this manuscript or similar manuscript has not been and will not be submitted to or published in any other publication before its appearance in the journal Construction and Building Materials. The authors transfer all copyright ownership of the aforementioned manuscript to the journal Construction and Building Materials.

### CRedit authorship contribution statement

**Mingke Deng:** Conceptualization, Methodology, Supervision, Funding acquisition, Project administration, Resources. **Tong Li:** Conceptualization, Methodology, Validation, Formal analysis, Investigation, Project administration, Resources, Writing - original draft, Writing - review & editing. **Yangxi Zhang:** Writing - review & editing.

### Declaration of Competing Interest

The authors declare that they have no known competing financial interests or personal relationships that could have appeared to influence the work reported in this paper.

### Acknowledgements

The investigation presented herein was supported by National Natural Science Foundation of China (Grant No. 51878545), Xi'an Science and Technology Bureau (Grant No. 20191522415K YPT015JC017) and Ministry of Housing and Urban-Rural Development of China (Grant No. 2019-K-043).

### References

- [1] W.S. McNary, D.P. Abrams, Mechanics of masonry in compression, *J. Struct. Eng.* 111 (4) (1985) 857–870.
- [2] H.B. Kaushik, D.C. Rai, S.K. Jain, Stress-strain characteristics of clay brick masonry under uniaxial compression, *J. Mater. Civil Eng.* 19 (9) (2007) 728–739.
- [3] M. Priestley, D.O. Bridgeman, Seismic resistance of brick masonry walls, *Bull. New Zealand Nat. Soc. Earthq. Eng.* 7 (4) (1974) 167–187.
- [4] B.D. Ewing, M.J. Kowalsky, Compressive behavior of unconfined and confined clay brick masonry, *J. Struct. Eng.* 130 (4) (2004) 650–661.
- [5] G. Campione, L. Cavaleri, M. Papia, Stainless steel grids for confinement of clay brick masonry columns, *J. Struct. Eng.* 142 (7) (2016) 04016038.
- [6] Y. Ouyang, N.K. Liu, Analysis of flexural behavior of masonry column strengthened by wrapped steel outside under axial compression, *Build. Struct.* 36 (11) (2006) 17–29 (in Chinese).

- [7] A. Borri, G. Castori, M. Corradi, Masonry confinement using steel cords, *J. Mater. Civil Eng.* 25 (12) (2013) 1910–1919.
- [8] G. Campione, L. Cavaleri, M. Papia, Brick masonry columns externally wrapped with steel wires under concentric and eccentric loads, *J. Mater. Civil Eng.* 29 (9) (2017) 04017125.
- [9] T.D. Kreaikas, T.C. Triantafyllou, Masonry confinement with fiber-reinforced polymers, *J. Compos. Constr.* 9 (2) (2005) 128–135.
- [10] M. Corradi, A. Grazini, A. Borri, Confinement of brick masonry columns with CFRP materials, *Compos. Sci. Technol.* 67 (9) (2007) 1772–1783.
- [11] M.A. Aiello, F. Micelli, L. Valente, FRP confinement of square masonry columns, *J. Compos. Constr.* 13 (2) (2009) 148–158.
- [12] V. Alecci, S.B. Bati, G. Ranocchiai, Study of brick masonry columns confined with CFRP composite, *J. Compos. Constr.* 13 (3) (2009) 179–187.
- [13] M. Di Ludovico, C. D'Ambra, A. Prota, G. Manfredi, FRP confinement of tuff and clay brick columns: experimental study and assessment of analytical models, *J. Compos. Constr.* 14 (5) (2010) 583–596.
- [14] C. Faella, E. Martinelli, S. Paciello, G. Camorani, M.A. Aiello, et al., Masonry columns confined by composite materials: experimental investigation, *Compos. B Eng.* 42 (2011) 692–704.
- [15] F. Micelli, R. Angiuli, P. Corvaglia, M.A. Aiello, Passive and SMA-activated confinement of circular masonry columns with basalt and glass fibers composites, *Compos. B Eng.* 67 (2014) 348–362.
- [16] K.S. Alotaibi, K. Galal, Axial compressive behavior of grouted concrete block masonry columns confined by CFRP jackets, *Compos. B Eng.* 114 (2017) 467–479.
- [17] H. El-Sokkary, K. Galal, Performance of eccentrically loaded reinforced-concrete masonry columns strengthened using FRP wraps, *J. Compos. Constr.* 23 (5) (2019) 04019032.
- [18] G. Minafò, J. D'Anna, C. Cucchiara, et al., Analytical stress-strain law of FRP confined masonry in compression: literature review and design provisions, *Compos. B Eng.* 115 (2017) 160–169.
- [19] I.A. Yilmaz, P.E. Mezrea, et al., External confinement of brick masonry columns with open-grid basalt reinforced mortar, in: *Proceedings of the Fourth Asia-Pacific Conference on FRP in Structures (APFIS 2013)*, Melbourne, Australia, 2013.
- [20] O.A. Cevallos, R.S. Olivito, R. Codispoti, L. Ombres, Flax and polyparaphenylene benzobisoxazole cementitious composites for the strengthening of masonry elements subjected to eccentric loading, *Compos. B Eng.* 71 (2015) 82–95.
- [21] G. Minafò, L. La Mendola, Experimental investigation on the effect of mortar grade on the compressive behaviour of FRP confined masonry columns, *Compos. B Eng.* 146 (2018) 1–12.
- [22] T.D. Kreaikas, Experimental study on carbon fiber textile reinforced mortar system as a means for confinement of masonry columns, *Constr. Build. Mater.* 208 (2019) 723–733.
- [23] M. Fossetti, G. Minafò, Comparative experimental analysis on the compressive behaviour of masonry columns strengthened by FRP, BFRM or steel wires, *Compos. B Eng.* 112 (2017) 112–124.
- [24] V.C. Li, S. Wang, C. Wu, Tensile strain-hardening behavior of PVA-ECC, *ACI Mater. J.* 98 (6) (2001) 483–492.
- [25] V.C. Li, On engineered cementitious composites (ECC)—a review of the material and its applications, *J. Adv. Concr. Technol.* 1 (3) (2003) 215–230.
- [26] T. Kanda, V.C. Li, Practical design criteria for saturated pseudo strain hardening behavior in ECC, *J. Adv. Concr. Technol.* 4 (1) (2006) 59–72.
- [27] K. Kobayashi, D.L. Ahn, K. Rokugo, Effects of crack properties and water-cement ratio on the chloride proofing performance of cracked SHCC suffering from chloride attack, *Cem. Concr. Compos.* 69 (2016) 18–27.
- [28] I. Curosu, V. Mechtcherine, D. Forni, E. Cadoni, Performance of various strain-hardening cement-based composites (SHCC) subject to uniaxial impact tensile loading, *Cem. Concr. Res.* 102 (2017) 16–28.
- [29] J.L. Kou, M.K. Deng, X.W. Liang, Experimental study of uniaxial tensile properties of ductile fiber reinforced concrete, *Build. Struct.* 43 (1) (2013) 59–64 (in Chinese).
- [30] M.K. Deng, M. Qin, X.W. Liang, Experimental study of compressive behavior of engineered cementitious composites, *Ind. Constr.* 45 (4) (2015) 120–126 (in Chinese).
- [31] M.K. Deng, J. Han, H.B. Liu, M. Qin, X.W. Liang, Analysis of compressive toughness and deformability of high ductile fiber reinforced concrete, *Adv. Mater. Sci. Eng.* 3 (2015) 1–7.
- [32] GB/T 2542-2012, Test Methods for Wall Bricks, Chinese Standard Press, Beijing, China, 2012 (in Chinese).
- [33] JGJ/T 70-2009, Standard for Test Method of Basic Properties of Construction Mortar, Chinese Building Industry Press, Beijing, China, 2009 (in Chinese).
- [34] M.K. Deng, W.B. Jing, M. Qin, X.W. Liang, Experimental research on compressive strength of high ductility fiber reinforced concrete, *Build. Struct.* 46 (23) (2016) 79–84 (in Chinese).
- [35] K.S. Alotaibi, K. Galal, Experimental study of CFRP-confined reinforced concrete masonry columns tested under concentric and eccentric loading, *Compos. B Eng.* 155 (2018) 257–271.
- [36] ACI Committee 440, Guide for the design and construction of externally bonded FRP systems for strengthening concrete structures ACI 440.2R-08. Farmington Hills, MI, 2008.
- [37] GB 50003-2011, Code for Design of Masonry Structures, Chinese Standard Press, Beijing, China, 2011 (in Chinese).
- [38] S.H. Cai, Z.S. Jiao, Behavior and ultimate strength of short concrete-filled steel tubular columns, *J. Build. Struct.* 6 (01) (1984) 32–40 (in Chinese).